Isospin dependence of projectile-like fragment production at intermediate energies

Ma Chun-Wang (马春旺),* Wei Hui-Ling (魏慧玲), Wang Jun-Yang (王俊阳), and Liu Gao-Jie (刘高杰)
College of Physics and Information Engineering, Henan Normal University, Xinxiang 453007, People's Republic of China

Fu Yao (傅瑶), Fang De-Qing (方德清), Tian Wen-Dong (田文栋), Cai Xiang-Zhou (蔡翔舟), Wang Hong-Wei (王宏伟), and Ma Yu-Gang (马余刚)
Shanghai Institute of Applied Physics, Chinese Academy of Sciences, P. O. Box 800-204, Shanghai 201800, People's Republic of China

(Received 20 October 2008; revised manuscript received 11 January 2009; published 18 March 2009)

The cross sections of fragments produced in 140 *A* MeV ^{40,48}Ca + ^{9}Be and ^{58,64}Ni + ^{9}Be reactions are calculated by the statistical abration-ablation (SAA) model and compared to the experimental results measured at the National Superconducting Cyclotron Laboratory (NSCL) at Michigan State University. The fragment isotopic and isotonic cross section distributions of ^{40}Ca and ^{48}Ca, ^{58}Ni and ^{64}Ni, ^{40}Ca and ^{58}Ni, and ^{48}Ca and ^{64}Ni are compared and the isospin dependence of the projectile fragmentation is studied. It is found that the isospin dependence decreases and disappears in the central collisions. The shapes of the fragment isotopic and isotonic cross section distributions are found to be very similar for symmetric projectile nuclei. The shapes of the fragment isotopic and isotonic distributions of different asymmetric projectiles produced in peripheral reactions are found to be very similar. The similarity of the distributions are related to the similar proton and neutron density distributions inside the nucleus in framework of the SAA model.

DOI: 10.1103/PhysRevC.79.034606 PACS number(s): 25.70.Mn, 21.65.Cd

I. INTRODUCTION

Projectile fragmentation is a well-established technique for the production of rare isotope beams used by many radioactive ion-beam facilities around the world. The process of projectile fragmentation has been studied extensively to investigate the reaction mechanisms in heavy ion collisions at intermediate and high energies. Understanding the physics of projectile fragmentation is important not only for rare-isotope beam production purposes but also for the fundamental nuclear physics processes involved in nuclear collisions [1–7].

Isospin effect is the phenomenon induced by the isospin degree of freedom in heavy-ion collisions. Isospin effects of various physical phenomena, such as multifragmentation, collective flow, preequilibrium nucleon emission, etc., have been reported [1,8–14]. These studies have shown that isospin effect exists in nuclear reactions induced by exotic nuclei but it may disappear under some conditions. In projectile fragmentation reactions, the yields of neutron-rich nuclei from fragmentation of neutron-rich projectiles will be larger than those from stable nuclei; this is one isospin effect in fragment production [14–17]. But the difference becomes smaller with the increase of the charge difference between the fragment and the projectile. And it may disappear at last. In Refs. [15] and [16], the fragment isotopic distributions of 60 *A* MeV ^{16,18}O + ^{9}Be, ^{36,40}Ar + ^{9}Be, and ^{40,48}Ca + ^{9}Be were presented by Fang *et al.* It was found that the peak position of isotopic distributions from stable nucleus induced reactions has a shift toward the neutron-rich side as compared to that from neutron-rich nucleus induced reactions. The shift becomes larger when the difference of neutron numbers of the two projectiles is bigger. This phenomena is called the isospin effect in the projectile fragmentation. But the isospin effect of fragmentation reaction on the isotopic distribution decreases with the increase of the atomic number difference and disappears at last.

In the campaign of four projectile fragmentation experiments carried out at the National Superconducting Cyclotron Laboratory (NSCL) at Michigan State University [18], eight different reaction systems and more than 1400 fragment cross sections have been measured. Reactions of primary 140 *A* MeV of ^{40}Ca, ^{48}Ca, ^{58}Ni, and ^{64}Ni colliding with light target ^{9}Be and heavy target ^{181}Ta were measured. Extensive study of the projectile fragmentation reactions using the EPAX code [18], the macroscopic-microscopic heavy ion phase space exploration (HIPSE) model, and the fully microscopic antisymmetrized molecular dynamics (AMD) model has been carried out [19]. With no variation of the model parameters, a reasonable agreement between the predictions and experimental data has been reached [19]. Comprehensive fragment cross sections of ^{40}Ca, ^{48}Ca, ^{58}Ni, and ^{64}Ni were presented in Refs. [18] and [19]. From the detailed cross section of fragments presented, it is possible to investigate the isospin effect of projectile fragmentation induced by the symmetric and asymmetric (neutron-rich) nuclei.

One of the methods used to calculate the cross section of fragments produced in projectile fragmentation is the statistical abrasion ablation (SAA) model. Compared to the HIPSE model and the AMD model, the calculation of the SAA model is simple and can reproduce the experimental results of heavy ion collision at intermediate energy well [15,17,20–22]. In this article, the cross section of fragments produced in 140 *A* MeV ^{40,48}Ca + ^{9}Be and ^{58,64}Ni + ^{9}Be reactions are calculated within the framework of the SAA model and compared to the NSCL experimental data [19]. The fragment

*machunwang@126.com

 ©2009 The American Physical Society

isotopic and isotonic cross section distributions between the four reactions is compared to study the isospin dependence of projectile-like fragmentation for symmetric and asymmetric nuclei.

II. THE SAA MODEL

The SAA model was developed by Brohm and Schmidt to describe the peripheral nuclear collisions at high energies in a picture of quasi-free nucleon-nucleon collisions [23]. It was modified by Fang and Zhong *et al.* to study the heavy ion collisions at intermediate energy [15,17,20–22,24]. The reactions in the SAA model are described as a two-step process. The initial stage can be described by a Glauber-type model as "participants" and "spectators." The participants in an overlapping region between the projectile and the target interact strongly while the spectators are left to move almost without being disturbed [25]. In the second evaporation stage, the system reorganizes because of excitation, which means that it is deexcited and thermalized by the cascade evaporation of light particles. After the deexcitation, the results of the final fragment, which are comparable to the experimental data, can be obtained. The details of the SAA model can be found in Refs. [15,20,23].

In the SAA model, the colliding nuclei are described to be composed of parallel tubes orienting along the beam direction. Neglecting the transverse motion, the collision is described by independent interactions of tube pairs. Assuming a binomial distribution for the absorbed projectile neutrons and protons in the interaction of a specific pair of tubes, the distributions of the total abraded neutrons and protons can be determined. For an infinitesimal tube in the projectile, the transmission probabilities for neutrons (protons) at a given impact parameter **b** are calculated by

$$t_k(\mathbf{s}-\mathbf{b}) = \exp\{-[D_n^T(\mathbf{s}-\mathbf{b})\sigma_{nk} + D_n^P(\mathbf{s}-\mathbf{b})\sigma_{pk}]\} \quad (1)$$

where D^T is the nuclear-density distribution of the target intergrated along the beam direction and normalized by $\int d^2s D_n^T = N^T$ and $\int d^2s D_p^T = Z^T$. N^T and Z^T refer to the neutron and proton numbers of the target, respectively. The vectors **s** and **b** are defined in the plane perpendicular to the beam. $\sigma_{k'k}$ is the free space nucleon-nucleon cross section ($k', k = n$ for neutron and $k', k = p$ for proton). The average absorbed mass in the limit to infinitesimal tubes at a given **b** is

$$\langle \Delta A(b)\rangle = \int d^2s D_n^T(\mathbf{s})[1 - t_n(\mathbf{s}-\mathbf{b})] + \int d^2s D_p^P(\mathbf{s})[1 - t_p(\mathbf{s}-\mathbf{b})]. \quad (2)$$

The excitation energy of the projectile spectator is estimated by the simple relation of $E^* = 13.3\langle \Delta A(b)\rangle$ MeV, where 13.3 is the mean excitation energy due to an abraded nucleon from the initial projectile [26].

The production cross section for a specific isotope can be calculated from

$$\sigma(\Delta N, \Delta Z) = \int d^2b P(\Delta N, b) P(\Delta Z, b), \quad (3)$$

where $P(\Delta N, b)$ and $P(\Delta Z, b)$ are the probability distributions for the abraded neutrons and protons at a given impact parameter b, respectively.

The σ of fragments produced in 140 A MeV ^{40,48}Ca + ^{9}Be and ^{58,64}Ni + ^{9}Be reactions are calculated within the framework of the SAA model. In the calculations, the free space nucleon-nucleon cross sections are adopted [27]. The proton and neutron density distributions are assumed to be the Fermi type,

$$\rho_i(r) = \frac{\rho_i^0}{1 + \exp\left(\frac{r - C_i}{t_i/4.4}\right)}, \quad i = n, p, \quad (4)$$

where ρ_i^0 is the normalization constant that ensures the integration of the density distribution equals the number of neutrons ($i = n$) or protons ($i = p$), t_i is the diffuseness parameter, and C_i is half the density radius of the neutron or proton density distribution.

III. RESULTS AND DISCUSSION

In Fig. 1, the σ of fragments produced in 140 A MeV ^{40,48}Ca + ^{9}Be reactions are plotted. In Fig. 2, the σ of fragments produced in ^{58,64}Ni + ^{9}Be reactions are plotted. The x axis is not the usually used mass number but the number of removed neutrons ($\Delta N = N_{\rm proj} - N_{\rm frag}$) for isotopes or the number of removed protons ($\Delta Z = Z_{\rm proj} - Z_{\rm frag}$) for isotones from the projectile, which not only can reflect the fine information of the reactions but also makes it convenient to compare between the fragment isotopic and isotonic distributions of different projectiles. From Figs. 1 and 2, it can be seen that the SAA model reproduces the experimental data quite well not only for the stable nucleus projectile but also for the neutron-rich nucleus projectile.

In Refs. [15] and [16], the fragment isotopic distributions of different projectiles are compared. The isospin effect and its disappearance in the projectile fragmentation is found. There is a shift from the fragment isotopic σ distributions (fragment isotopic distribution) of ^{40}Ca to that of ^{48}Ca. There is also a shift from the isotonic σ distributions of ^{40}Ca to that of ^{48}Ca. It is the same phenomena as observed in Refs. [15] and [16]; i.e., for the neutron-rich projectile, neutrons are more easily removed than for the symmetric nucleus projectile.

For ^{40}Ca, in Fig. 1, the shapes of the fragment isotopic and isotonic distributions are similar but there is a shift from the isotopic to the isotonic distributions. The shift indicates the isospin dependence of the fragment production. The shift becomes smaller when ΔZ of fragment isotopes and ΔN of fragment isotones increases, which means that central collisions begin to dominate the reactions. In other words, the isospin effect decreases in central collisions. The fragment isotopic distributions of ^{48}Ca are wider than those of ^{40}Ca. It is easy to understand because ^{48}Ca is a neutron-rich nucleus and has a neutron skin structure, from which neutrons can be removed more easily. The shift between the fragment isotopic and isotonic distributions of ^{48}Ca is in the reverse direction of that of ^{40}Ca and become wider compared to those of ^{40}Ca, which indicates that the isospin effect in ^{48}Ca projectile

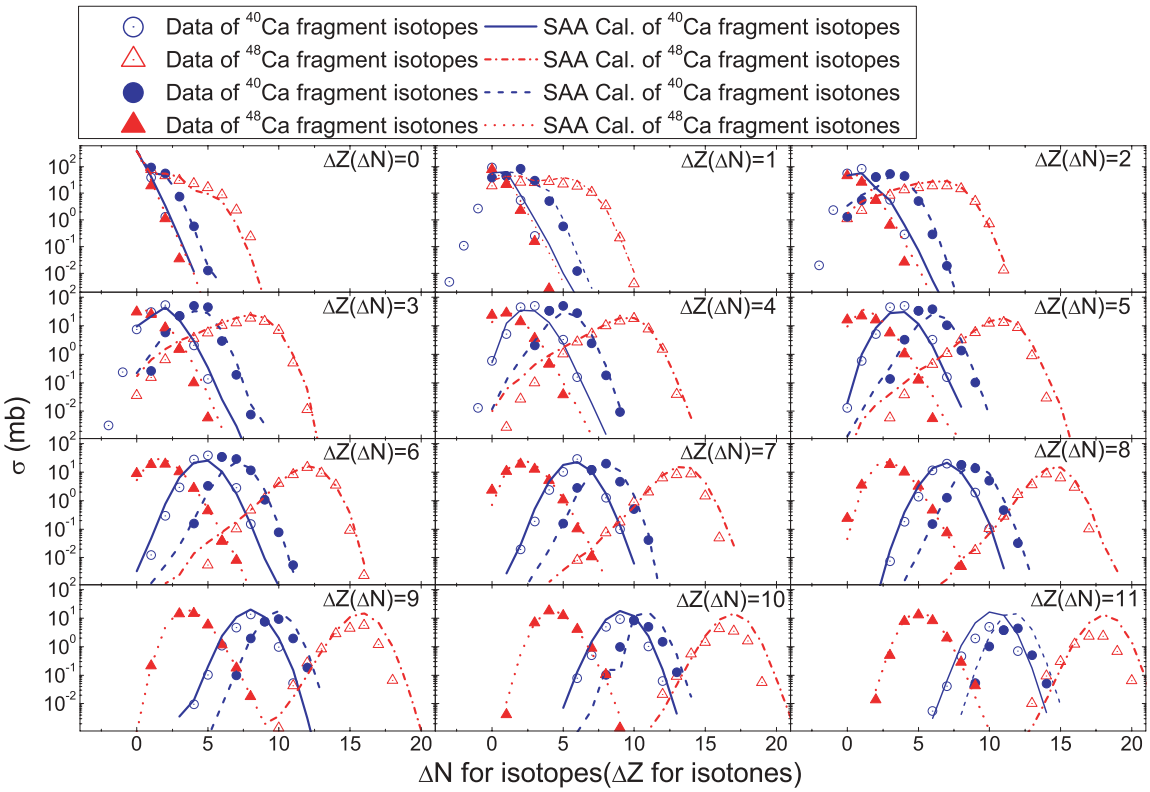

FIG. 1. (Color online) The cross sections of fragments produced in the 140 A MeV ^{40,48}Ca + ^{9}Be reactions. The open circles denote the fragment isotopic σ distributions and the solid ones denote the fragment isotonic σ distributions of the ^{40}Ca + ^{9}Be reaction. The x axis represents the numbers of protons removed ($\Delta Z = Z_{\rm proj} - Z_{\rm frag}$) from the projectile for the isotones and the numbers of neutrons removed ($\Delta N = N_{\rm proj} - N_{\rm frag}$) from the projectile for the isotopes in the pad. The open triangles denote the fragment isotopic σ distributions and the solid triangles denote the fragment isotonic σ distributions of ^{48}Ca + ^{9}Be reaction. The lines are the results of the SAA model calculations.

fragmentation does not decrease but is enhanced in central collisions.

The shapes of fragment isotopic and isotonic distributions of ^{58}Ni are similar to those of ^{40}Ca. The fragment isotopic and isotonic distributions of ^{64}Ni are similar to those of ^{48}Ca. What interested us most in Fig. 2 is that the fragment isotopic and isotonic distributions overlap when ΔZ of isotopes and ΔN of isotones are more than 9. It is the direct evidence of the disappearance of the isospin dependence of the projectile fragmentation. Compared to that of ^{40}Ca, it also means there is less isospin dependence in the projectile fragmentation of ^{58}Ni.

From the investigations of the fragment isotopic and isotonic distributions of ^{40}Ca and ^{58}Ni, evidence for the decrease and disappearance of the isospin effect in projectile fragmentation is found; i.e., the shift from the fragment isotopic distributions to the fragment isotonic distributions of ^{40}Ca and ^{58}Ni becomes narrower and the fragment isotopic and isotonic distributions of ^{58}Ni overlap.

There is little difference between the proton and neutron density distributions inside the symmetric nucleus. For ^{40}Ca and ^{58}Ni, with N/Z equal to 1.0 and 1.071, respectively, the proton and neutron density distributions should be very similar, except the size of ^{58}Ni is larger than that of ^{40}Ca. There are some reasons to expect similar fragment isotopic and isotonic distributions of their projectile fragmentation. In Fig. 3, the σ values of fragments produced in ^{40}Ca/^{58}Ni + ^{9}Be reactions are plotted. Though the fragment isotopic distribution of ^{40}Ca is narrower than that of ^{58}Ni, the difference between the fragment isotopic distributions of ^{40}Ca and ^{58}Ni is small. The same behavior is exhibited in the fragment isotonic distributions. Because the difference between ^{40}Ca and ^{58}Ni mass numbers is not very big, it can be concluded that, for symmetric projectile nuclei with similar mass numbers, the fragment isotopic and isotonic distributions should be similar. Studying these distributions more carefully, it can be seen that the σ values of fragments produced in peripheral reactions of ^{40}Ca and ^{58}Ni have less difference than those in central collisions. For the $\Delta Z \geqslant 3$ isotopes, the σ values of fragments of ^{58}Ni are higher than those of ^{40}Ca on the right sides of the distributions while the left sides of the distributions show very little difference. For the $\Delta N \geqslant 3$ isotones, the σ values of fragments of ^{58}Ni are higher than those of ^{40}Ca on the left sides of the distributions while the right sides of the distributions show very little difference.

In Fig. 4, the σ values of fragments produced in ^{48}Ca/^{64}Ni + ^{9}Be reactions are plotted. There is very little difference between the fragment isotopic distributions of ^{48}Ca

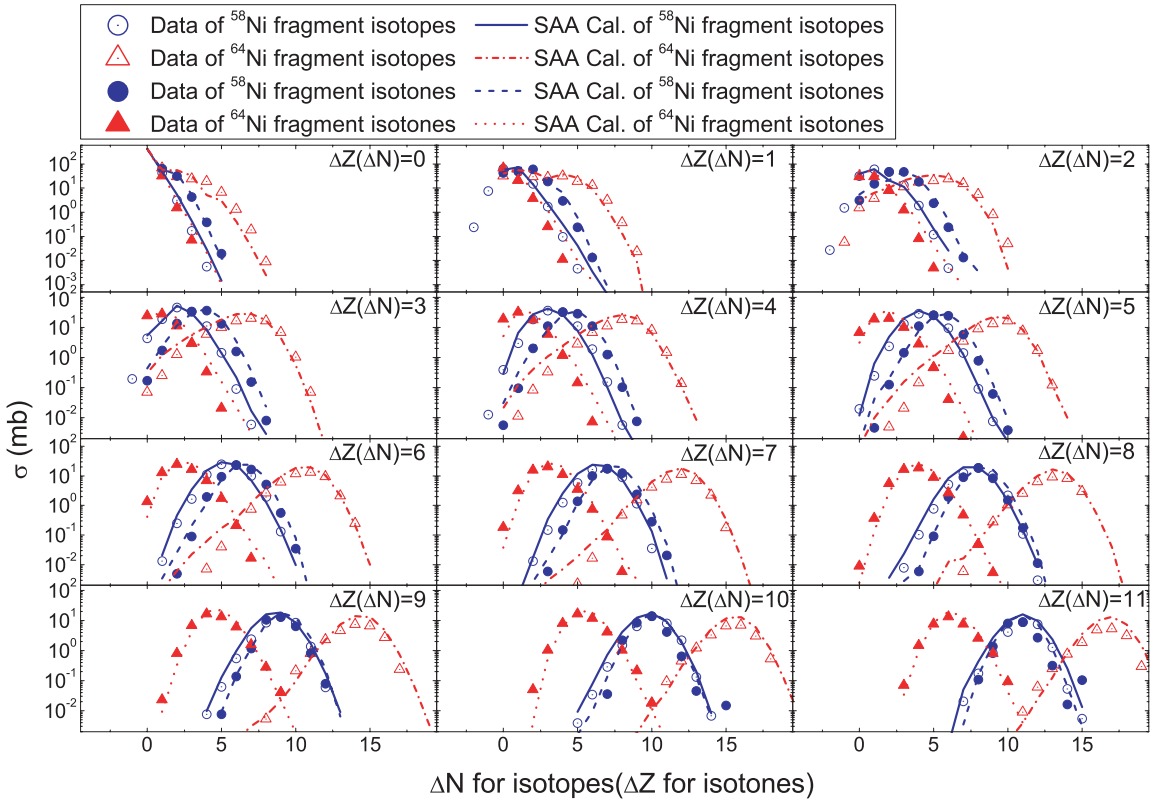

FIG. 2. (Color online) The cross sections of fragments produced in the 140 A MeV ^{58,64}Ni + ^{9}Be reactions. The open circles denote the fragment isotopic σ distributions and the solid ones denote the fragment isotonic σ distributions of the ^{58}Ni + ^{9}Be reaction. The x axis represents the numbers of protons removed ($\Delta Z = Z_{\rm proj} - Z_{\rm frag}$) from the projectile for the isotones and the numbers of neutrons removed ($\Delta N = N_{\rm proj} - N_{\rm frag}$) from the projectile for the isotopes in the pad. The open triangles denote the fragment isotopic σ distributions and the solid triangles denote the fragment isotonic σ distributions of the ^{64}Ni + ^{9}Be reaction. The lines denote the results of the SAA model calculations.

and ^{64}Ni in peripheral reactions. For the $\Delta Z < 3$ isotopes, though the right sides (more nucleons removed) of the isotopic distributions have a shift from the fragments of ^{48}Ca to ^{64}Ni, the left sides (little nucleons removed) of the isotopic distributions show very little difference. The $\Delta N < 3$ isotones of ^{48}Ca and ^{64}Ni overlap. The fragments on the left side of the $\Delta Z < 3$ isotopes and the $\Delta N < 3$ isotones are the productions of most peripheral reactions. In Fig. 4, the shapes of the $\Delta Z \geqslant 3$ isotopic distributions of ^{48}Ca and ^{64}Ni are very similar but the isotopic distributions of ^{48}Ca shift to those of ^{64}Ni and the right sides of the distributions overlap gradually. Compared to the left side of the distribution, the right side of the distribution means that the central collisions happen most. For ^{48}Ca and ^{64}Ni, the distributions of $\Delta Z \leqslant 5$ fragment isotones, which are the productions in peripheral reactions, show very little difference.

By investigating the fragment distributions of the four projectiles, the isospin effect in the projectile fragmentation is exhibited. By comparing the fragment isotopic and isotonic distributions of ^{40}Ca and ^{58}Ni, it has been found that the isospin dependence of the projectile fragmentation decreases and disappears. The similarities of the fragment isotopic and isotonic distributions from projectile fragmentation are discovered not only in symmetric nuclei but also in asymmetric nuclei. It is meaningful to discover the similarities of the fragment isotopic and isotonic distributions because it help us to estimate the production of fragments in projectile fragmentation at intermediate energy. But why do these phenomena happen?

According to the SAA model, the number of protons or neutrons removed in a specific pipe in collision is determined by the nucleon-nucleon cross section and the densities of the protons and neutrons. Because the projectile fragmentation of ^{40,48}Ca and ^{58,64}Ni occur under the same experimental conditions, the deexcitation in the reactions is the same and there is no need to consider the target effect in the reactions. Some qualitative explanations of the phenomena observed above can be obtained from the SAA model.

For symmetric nuclei, their proton and neutron density distributions are similar. According to the SAA model, the fragment isotopic and isotonic distributions of projectile fragmentation should be similar and the difference should reflect the difference in the proton and neutron distributions. The shift from the fragment isotopic distribution to the isotonic distribution in peripheral reactions of ^{40}Ca reveals the difference in the proton and neutron density distributions in the surface

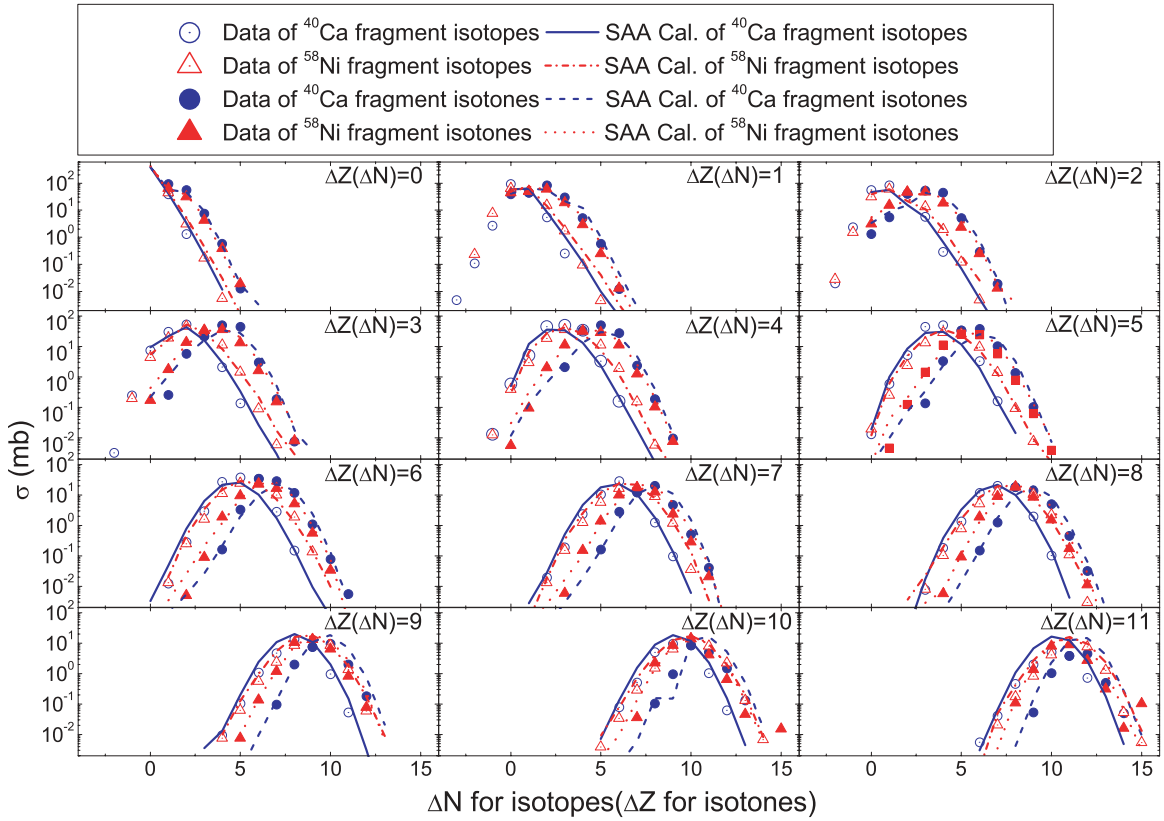

FIG. 3. (Color online) The cross sections of fragments produced in the 140 A MeV ^{40}Ca + ^{9}Be and ^{58}Ni + ^{9}Be reactions. The open circles denote the fragment isotopic σ distributions and the solid ones denote the fragment isotonic σ distributions of the ^{40}Ca + ^{9}Be reaction. The open triangles denote the fragment isotopic σ distributions and the solid triangles denote the fragment isotonic σ distributions of the ^{58}Ni+^{9}Be reaction. The lines denote the results of the SAA model calculations.

region. It should be kept in mind that even in the central collisions the surface effect of the nucleus also exists because, in a specific pipe involved in collisions, the density distribution is the mixed effect of the surface and the core. But the surface effect decreases in the central collision because the density of the core will wash out some density difference in the surface region. It makes the shift from fragment isotopic distributions to isotonic distributions become smaller. For ^{58}Ni, the surface effect becomes unimportant in most central collisions, which results in the overlap of the fragment isotopic and isotonic distributions.

For asymmetric neutron-rich nuclei that have a very large N/Z value, more neutrons are pushed to the surface region and there is a neutron skin structure. In the surface region, the neutron density is bigger than the proton density and the proton-removing will be more difficult than the neutron-removing in peripheral reactions. The wide spread of the fragment isotopic distributions of ^{48}Ca and ^{64}Ni in the top three panels of Fig. 4 is the evidence for that. For ^{48}Ca and ^{64}Ni, with N/Z equals 1.4 and 1.286, respectively, there should be a difference in their neutron density. The similar shapes of the $\Delta N < 3$ fragment isotonic distributions of ^{48}Ca and ^{64}Ni reveal the similar proton density distributions in the surface regions of ^{48}Ca and ^{64}Ni, while the shift on the right sides of the distributions maybe due to the different diffuseness of ^{48}Ca and ^{64}Ni according to Ref. [28]. The similarity of the left parts of the fragment isotopic distributions reveals the similarity of the neutron density distributions in the surface regions of ^{48}Ca and ^{64}Ni while the shift from the fragment isotopic distributions of ^{64}Ni to those of ^{48}Ca reveals the difference of the neutron density distributions between them.

IV. SUMMARY

In summary, by investigating the fragment isotopic and isotonic cross section distributions of 140 A MeV ^{40,48}Ca + ^{9}Be and ^{58,64}Ni + ^{9}Be reactions, evidence of the isospin effect and its disappearance in projectile fragmentation has been found. Some similarity of the fragment isotopic and isotonic distributions between not only symmetric nuclei but also asymmetric (neutron-rich) nuclei has been found. These similarities are related to the similar proton and neutron density distributions in the framework of the SAA model. These similarities will help to estimate the fragment production in heavy ion collisions at intermediate energy.

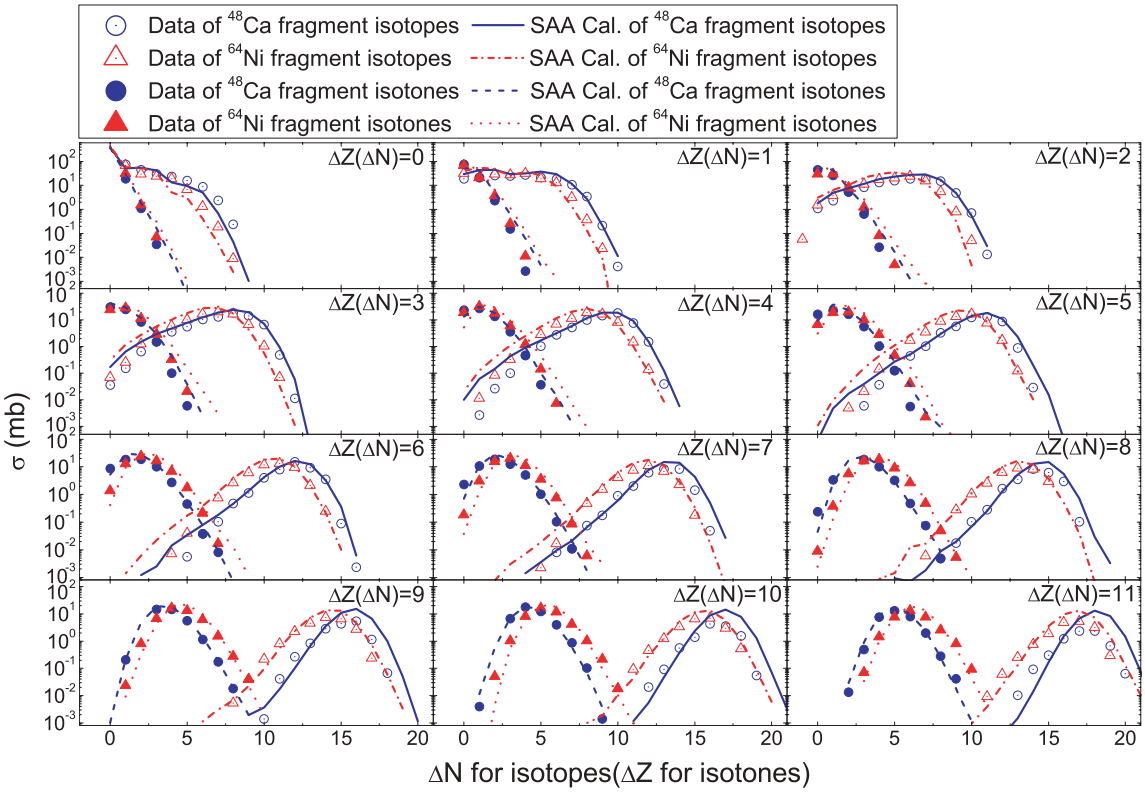

FIG. 4. (Color online) The cross sections of fragments produced in the 140 A MeV ^{48}Ca + ^{9}Be and ^{64}Ni + ^{9}Be reactions. The open circles denote the fragment isotopic σ distributions, and the solid ones denote the fragment isotonic σ distributions of the ^{48}Ca + ^{9}Be reaction. The open triangles denote the fragment isotopic σ distributions and the solid triangles denote the fragment isotonic σ distributions of the ^{64}Ni + ^{9}Be reaction. The lines denote the results of the SAA model calculations.

ACKNOWLEDGMENTS

This work was partially supported by the National Science Foundation of China (Grants No. 10775168 and 10775039), the State Key Program of Basic Research of China (Grant No. 2007CB815004), and Shanghai Development Foundation for Science and Technology (Grant No. 06QA14062).

[1] B. A. Li, Z. Ren, C. M. Ko, and S. J. Yennello, Phys. Rev. Lett. **76**, 4492 (1996).

[2] B. A. Brown, Phys. Rev. Lett. **85**, 5296 (2000).

[3] M. B. Tsang, W. A. Friedman, C. K. Gelbke, W. G. Lynch, G. Verde, and H. Xu, Phys. Rev. Lett. **86**, 5023 (2001).

[4] Y. G. Ma, A. Siwek, J. Peter *et al.*, Phys. Lett. **B390**, 41 (1997).

[5] Y. G. Ma, J. B. Natowitz, R. Wada *et al.*, Phys. Rev. C **71**, 054606 (2005).

[6] J. A. Hauger, P. Warren, S. Albergo *et al.*, Phys. Rev. C **57**, 764 (1998).

[7] Y. G. Ma, T. Z. Yan, X. Z. Cai, J. G. Chen, D. Q. Fang, W. Guo, G. H. Liu, C. W. Ma, E. J. Ma, W. Q. Shen, Y. Shi, Q. M. Su, W. D. Tian, H. W. Wang, and K. Wang, Nucl. Phys. **A787**, 611c (2007).

[8] J. F. Dempsey, R. J. Charity, L. G. Sobotka, G. J. Kunde, S. Gaff, C. K. Gelbke, T. Glasmacher, M. J. Huang, R. C. Lemmon, W. G. Lynch, L. Manduci, L. Martin, M. B. Tsang, D. K. Agnihotri, B. Djerroud, W. U. Schroder, W. Skulski, J. Toke, and W. A. Friedman, Phys. Rev. C **54**, 1710 (1996).

[9] R. Pak, W. Benenson, O. Bjarki, J. A. Brown, S. A. Hannuschke, R. A. Lacey, Bao-An Li, A. Nadasen, E. Norbeck, P. Pogodin, D. E. Russ, M. Steiner, N. T. B. Stone, A. M. Vander Molen, G. D. Westfall, L. B. Yang, and S. J. Yennello, Phys. Rev. Lett. **78**, 1022 (1997).

[10] R. Pak, B. A. Li, W. Benenson, O. Bjarki, J. A. Brown, S. A. Hannuschke, R. A. Lacey, D. J. Magestro, A. Nadasen, E. Norbeck, D. E. Russ, M. Steiner, N. T. B. Stone, A. M. Vander Molen, G. D. Westfall, L. B. Yang, and S. J. Yennello, Phys. Rev. Lett. **78**, 1026 (1997).

[11] C. Liewen, Z. Fengshou, and J. Genming, Phys. Rev. C **58**, 2283 (1998).

[12] S. Kumar, M. K. Sharma, R. K. Puri, K. P. Singh, and I. M. Govil, Phys. Rev. C **58**, 3494 (1998).

[13] Ma Yugang, Acta Phys. Sin. **49**, 654 (2000) (in Chinese).

[14] M. L. Miller, O. Bjarki, D. J. Magestro, R. Pak, N. T. B. Stone, M. B. Tonjes, A. M. Vander Molen, G. D. Westfall, and W. A. Friedman, Phys. Rev. Lett. **82**, 1399 (1999).

[15] D. Q. Fang, W. Q. Shen, J. Feng, X. Z. Cai, J. S. Wang, Q. M. Su, Y. G. Ma, Y. T. Zhu, S. L. Li, H. Y. Wu, Q. B. Gou, G. M. Jin, W. L. Zhan, Z. Y. Guo, and G. Q. Xiao, Phys. Rev. C **61**, 044610 (2000).

[16] Fang De-Qing, Shen Wen-Qing, Feng Jun, Cai Xiang-Zhou, Wang Jian-Song, Su Qian-Min, Ma Yu-Gang, Zhu Yong-Tai,

Li Song-Lin, Wu He-Yu, Gou Quan-Bu, Jin Gen-Ming, Zhan Wen-Long, Guo Zhong-Yan, and Xiao Guo-Qing, Chin. Phys. Lett. **17**, 267 (2000).

[17] D. Q. Fang, W. Q. Shen, J. Feng, X. Z. Cai, Y. G. Ma, H. Y. Zhang, P. Y. Hu, W. L. Zhan, Z. Y. Guo, G. Q. Xiao, J. X. Li, M. Wang, J. F. Wang, Z. J. Ning, J. Q. Wang, J. S. Wang, Q. J. Wang, and Z. Q. Chen, Eur. Phys. J. A **10**, 381 (2001).

[18] M. Mocko, M. B. Tsang, L. Andronenko, M. Andronenko, F. Delaunay, M. Famiano, T. Ginter, V. Henzl, D. Henzlova, H. Hua, S. Lukyanov, W. G. Lynch, A. M. Rogers, M. Steiner, A. Stolz, O. Tarasov, M.-J. van Goethem, G. Verde, W. S. Wallace, and A. Zalessov, Phys. Rev. C **74**, 054612 (2006).

[19] M. Mocko, M. B. Tsang, D. Lacroix, A. Ono, P. Danielewicz, W. G. Lynch, and R. J. Charity, Phys. Rev. C **78**, 024612 (2008).

[20] Fang Deqing, Feng Jun, Shen Wenqing, Cai Xiangzhou, Wang Jiansong, Ye Wei, and Ma Yugang, High Energy Phys. Nucl. Phys. **23**, 475 (1999) (in Chinese).

[21] C. Zhong, Y. G. Ma, D. Q. Fang, X. Z Cai, J. G. Chen, W. Q. Shen, W. D. Tian, K. Wang, Y. B. Wei, J. H. Chen, W. Guo, C. W. Ma, G. L. Ma, Q. M. Su, T. Z. Yan, and J. X. Zuo, Chin. Phys. **15**, 1481 (2006).

[22] C. Zhong, D. Q. Fang, X. Z. Cai, W. Q. Shen, H. Y. Zhang, Y. B. Wei, and Y. G. Ma, High Energy Phys. Nucl. Phys. **27**, 39 (2003) (in Chinese).

[23] T. Brohm and K.-H. Schmidt, Nucl. Phys. **A569**, 821 (1994).

[24] Ma Chun-Wang, Fu Yao, Fang De-Qing, Ma Yu-Gang, Cai Xiang-Zhou, Guo Wei, Tian Wen-Dong, and Wang Hong-Wei, Chin. Phys. B **17**, 1216 (2008).

[25] Y. Eisenberg, Phys. Rev. **52** 1378 (1954).

[26] J. J. Gaimard and K.-H. Schmidt, Nucl. Phys. **A531**, 709 (1991).

[27] Cai Xiangzhou, Feng Jun, Shen Wenqing, Ma Yugang, Wang Jiansong, and Ye Wei, Phys. Rev. C **58**, 572 (1998).

[28] A. Trzcinska, J. Jastrzebski, P. Lubinnski, F. J. Hartmann, R. Schmidt, T. V. Edigy, and B. Klos, Phys. Rev. Lett. **87**, 082501 (2001).